A Study of Acoustic Emission from Sandy Soils

Etude sur l'Emission Acoustique de Sols Sableux

K.TANIMOTO Professor,
T.NODA Assistant, Department of Civil Engineering, Kobe University, Japan

SYNOPSIS Acoustic emission from sandy soils is observed during triaxial compression tests, to establish a method of predicting the failure life of soils by emission counts. Emission rate, an index which is hardly affected by the sensitivity of monitoring devices, is defined by the characteristics of emission counts monitored during tests. The correlation between emission rate and failure life is simple and unique regardless of soil type, confined stress, water content and dry density of samples, the rate of strain in strain controlled tests and the rate of loading in stress controlled tests. Therefore it may be possible to apply this correlation to practical problems in which failure life of soils is of importance.

INTRODUCTION

The techniques of monitoring acoustic emission have been used not only in the study of rock materials related to earthquake modeling, landslides and slope failure (for example, Mogi 1962, Sholz 1968, Hardy 1973), but also in the study of various metals with growing cracks to fracture (Gerberich et al. 1967, Tetelman et al. 1972). Emission has also been observed in concrete, wood, plastics etc. However, little work done in soil mechanics has so far been reported (Hakuno et al. 1969, Koerner et al. 1972).

Acoustic emission is generated as a result of the release of kinetic energy from internal deformation in stressed materials, and the energy level and the frequency characteristics could be dependent on test materials with different structures. Accordingly, significantly different technique is required for each material. In sandy soils during shear, emission is supposed to be generated at relatively low level of energy and frequency from interparticle friction in the beginning of shearing, and at relatively high level in catastrophic deformation at failure. Therefore, the characteristics of emissions monitored during the entire range of shearing may give a possible means to explore internal structure in deformation process and to predict the time to failure.

METHOD OF EXPERIMENT

The experimental setup consists of a triaxial compression apparatus, emission recording units and emission analysing units, as shown in Fig. 1. The loading method by water feed is employed in stress controlled tests to avoid noise by a drive motor, and the loading part is modified to allow hand-operated strain controlled tests when necessary. A piezoelectric transducer is accommodated on the base plate in the cell. Emission monitored by the transducer is recorded by a data recorder, which allows to replay at a suitable speed for analysing process.

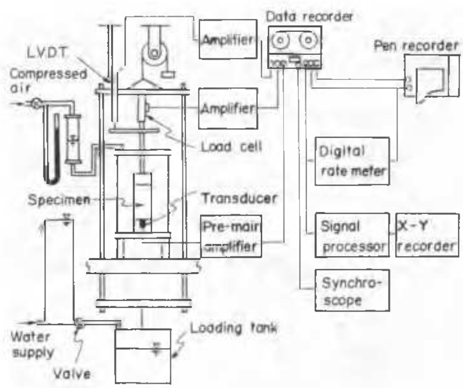

Fig. 1 Experimental setup for monitoring and analysing acoustic emission.

Test soils are well-graded sands from different origins of decomposed granite. The two series of tests, stress controlled and strain controlled, are carried out under drained condition for unsaturated samples. Test conditions are listed in Table I.

ACOUSTIC EMISSION IN STRAIN CONTROL TESTS

Acoustic emission observed during tests are a group of transient vibrations of various amplitudes and frequencies. Therefore, emis-

Table I Test conditions

Type of test	Strain control	Stress control	
Loading speed ($\dot{\sigma}_d$)		$0.02 \sim 1.22$ kg/cm²/min	
Strain rate ($\dot{\varepsilon}$)	$0.17 \sim 3.36$ %/min		
Confined stress (σ_3)	0.5, 1.5 kg/cm²	0.5, 1.0, 1.5 kg/cm²	
Test soils	S − 1	S − 1	S − 2
Maximum grain size	4.76 mm	Same as the left column	9.52 mm
Effective grain size	0.105 mm		0.205 mm
Uniformity coefficient	16.8		8.2
Consistency	NP		NP
Water content (w)	$1 \sim 8$ %	$0 \sim 14$ %	
Dry density (γ_d)	$1.51 \sim 1.76$ g/cm³	$1.53 \sim 1.75$ g/cm³	
Transducer	DC $\sim$ 40 kHz		
Pre-main amplifier	60 dB, 100 kHz − 3 dB		
Data recorder	Max. 15 ips, $10 \sim 6 \times 10^4$ Hz ± 3 dB		
Digital rate meter	Discri. 0~5 V, Sample rate 1~60 sec		

sion count depends on a discrimination level. In this study, a discrimination level of 1.0 volt is employed at the input to the digital rate meter to cut off background noise.

Fig. 2 shows the plots of emission count per minute (n_e) on a stress-strain diagram. It is noted from this figure that the emission

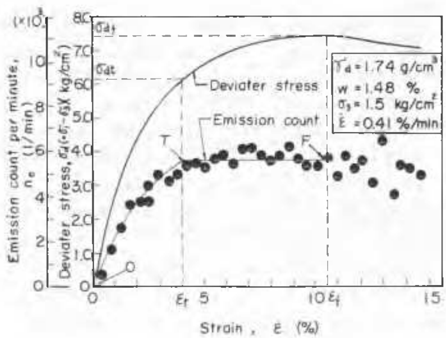

Fig. 2 Emission count per minute, deviator stress and axial strain relationship in strain control tests.

count increases with the strain growth during the first process from the point 0 to the point T, but becomes nearly constant during the second process from T to F at the time of failure. It is considered that steady-state interparticle friction occurs during the latter process.

To find the position of T, peculiar in the entire range of a test, the relationship between σ_{dt}/σ_{df} and $\varepsilon_t/\varepsilon_f$ in all the strain control tests is drawn in Fig. 3, where σ_{dt}, ε_t, σ_{df} and ε_f denote deviator stresses and axial strains corresponding to T and F, respectively. The dispersion of the plots are

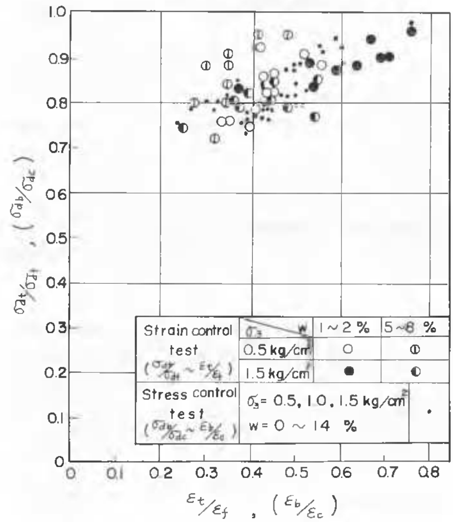

Fig. 3 Relationship between σ_{dt}/σ_{df} and $\varepsilon_t/\varepsilon_f$ in strain control tests and relationship between σ_{db}/σ_{dc} and $\varepsilon_b/\varepsilon_c$ in stress control tests.

not so large for specified combination of confined stress and water content in tests.

In the steady-state process, the constancy of emission count per minute is supposed to be connected with the constant rate of strain. To see this the relationship betweer emission count during this process and strain rate in all the strain control tests is drawn in Fig. 4. It is noted from this figure that emission count is approximately proportional to strain rate.

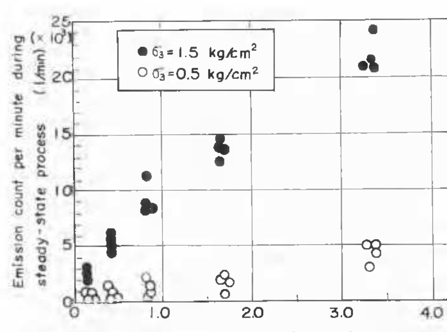

Fig. 4 Relationship between strain rate and emission count per minute monitored during steady-state process of strain control tests.

ACOUSTIC EMISSION IN STRESS CONTROL TESTS

A typical result of stress control tests is shown in Fig. 5, from which it can be seen that emission count increases slowly with strain growth until the strain attains a certain magnitude, and promptly increases after exceeding that value. Thus the entire range is made of two distinct processes, from 0 to B and from B to C at failure. The rapid increase in emission count in the latter process may be related to the quick rate of strain likely developed before failure.

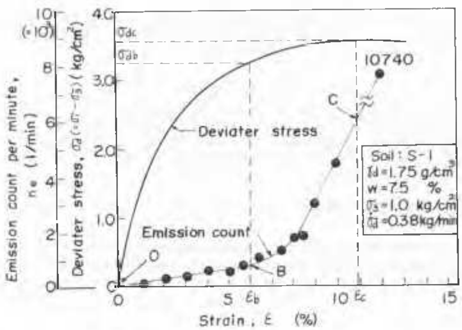

Fig. 5 Emission count per minute, deviator stress and axial strain relationship in stress control test.

Let denote deviator stresses and axial strains at B and C by σ_{db} , ε_b , σ_{dc} and ε_c , respectively. Then the relationship between σ_{db}/σ_{dc} and $\varepsilon_b/\varepsilon_c$ is given by the plots of small circles in Fig. 3. Though rather scattered, the plots are, as a whole, similar to those in strain control tests, which may suggest that the point B corresponds to the point T.

PREDICTION OF FAILURE TIME

The creep-rupture life of cohesive soils has been studied in previous papers (for example, Murayama et al. 1956, Saito et al. 1961), in which a parameter of prime importance was strain rate. Since strain rate is, as seen in Fig. 4, nearly proportional to emission count during the steady-state process of strain control tests, it may be possible to predict failure time by emission count.

The correlation of emission count per minute (n_e) during steady-state process with time to failure from the start of tests (t_f) is given by Fig. 6. The figure shows that n_e-t_f relationships are approximately linear to logarithmic scales, and are independent of strain rate, water content and dry density of samples, but not of confined stress. Another problem of this relationships is that emission count is necessarily changeable with the sensitivity of monitoring devices and a location where a transducer is set.

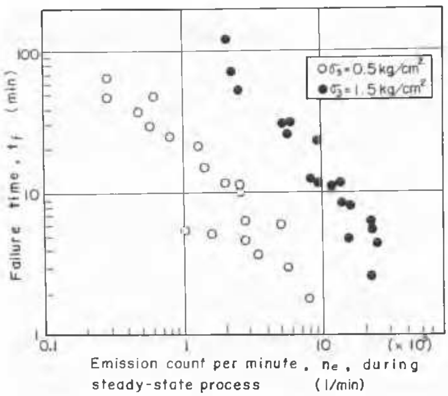

Fig. 6 Prediction of failure time by emission count per minute monitored during steady-state process of strain control tests.

To get an improved correlation, an index, emission rate R, is defined as illustrated in an emission count-time domain in the corner of Fig. 7, where

N: total emission count observed during the first process,

ΔN: emission count observed in a small period (30 sec in the following) directly after the end of the first process, and

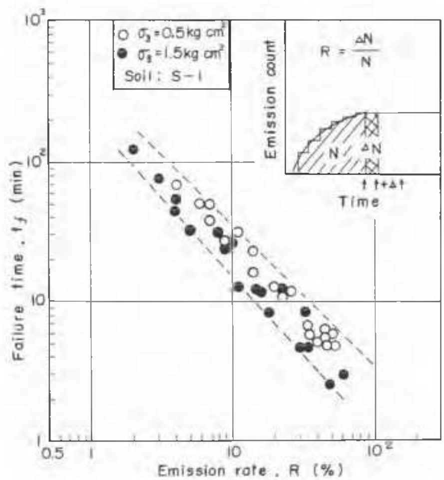

Fig. 7 Prediction of failure time by emission rate in strain control tests.

$$R \text{ (emission rate)} = \Delta N/N \quad .....(1)$$

The correlation of R and t_f is given by Fig. 7, which shows a good linearity independent of confined stress as well as the rate of strain, water content and dry density of the samples in strain control tests. Of more interest is that this correlation is hardly affected by the sensitivity of monitoring devices and a discrimination level employed.

Emission rate in stress control tests can also be defined by the same expression as in the above, and is illustrated in the corner of Fig. 8. Thus R-t_f relationship can be obtained, as shown in Fig. 8. This relationship is also linear regardless of soil type, loading rate and soil conditions in all the stress control tests.

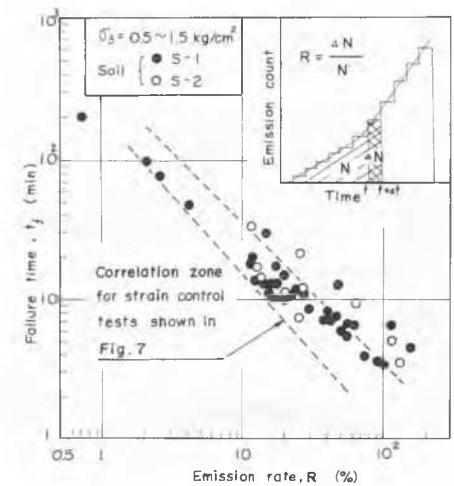

Fig. 8 Prediction of failure time by emission count in stress control tests.

Two broken lines in Fig. 8 indicate the correlation zone for the strain control tests, transferred from Fig. 7. The regression lines for both the correlations are approximately expressed by

$$\log_{10} t_f = -0.98 \log_{10} R + 2.36 \quad ...(2)$$

for the strain control tests, and

$$\log_{10} t_f = -0.88 \log_{10} R + 2.30 \quad ...(3)$$

for the stress control tests, where t_f is measured in minute. Since eqs. (2) and (3) are not much different from each other, a rough average expression:

$$\log_{10} t_f = -0.95 \log_{10} R + 2.35 \quad ...(4)$$

may be applicable to both the types of tests.

CONCLUSIONS

From the results described in the above, it may be concluded that:

The entire range of a shear test is composed of two distinct processes in view of the characteristics of acoustic emission, although the processes are in different forms for each of strain controlled tests and stress controlled tests.

Emission count observed during steady-state process in strain controlled tests is nearly proportional to strain rate.

Failure time t_f can be predicted by emission rate R defined by eq. (1), regardless of soil type, confined stress, water content and dry density of samples, strain rate in strain controlled tests and loading rate in stress controlled tests.

ACKNOWLEDGEMENTS

The authors wish to thank Messrs. H. Noguchi, A. Tanaka and Y. Nakashiba for their assistance during the progress of this research.

REFERENCES

Gerberich, W.W. and C.E. Hartbower(1967), "Some Observations on Stress Wave Emission as a Measure of Crack Growth," Int. Jnl. of Fracture Mech., Vol. 3, pp. 185-192.

Hakuno, M. et al.(1969),"Analysis of Noise Generated by Sand Particles when They Slide", Trans. JSCE, No. 164, pp.51-58(in Japanese).

Hardy, H.R.Jr.(1973),"Microseismic Techniques-Basic and Applied Research," Rock Mech., Springer-Verlag, Suppl. 2, pp. 93-114.

Koerner, R.M. and A.E. Lord Jr.(1972),"Acoustic Emission in Medium Plasticity Clayey Silt,"Proc. ASCE, Vol. 98, No. SM 1, pp. 161-165.

Mogi, K.(1962),"Study of Elastic Shocks Caused by the Fracture of Hetrogeneous Materials and its Relations to Earthquake Phenomena," Bull. Earthq. Res. Inst., Univ. of Tokyo, Vol. 40, pp. 125-173.

Murayama, S. and T. Shibata(1956),"On the Rheological Characteristics of Clay," Trans. JSCE, No.40, pp. 1-31(in Japanese).

Saito, M. and H. Uezawa(1961),"Failure of Soil Due to Creep," Proc. 5th ICSMFE, Vol. 1, pp. 315-318.

Sholz, C.H.(1968),"The Frequency-Magnitude Relation of Microfracturing in Rock and its Relation to Earthquake," Bull. Seism. Soc. of America, Vol. 58, No. 1, pp. 399-415.

Tetelman, A.S. and R. Chow(1972),"Acoustic Emission and Microcracking Processes,"Acoustic Emission, ASTM STP-505, pp. 30-40.